Identification of orthotropic membranes with high stiffness ratio

Computational Mechanics /

Identification of orthotropic membranes with high stiffness ratio

M.R. van Ratingen

IDENTIFICATION OF ORTHOTROPIC MEMBRANES WITH HIGH STIFFNESS RATIO

M.R. van Ratingen

Computational Mechanics / Department of Engineering Fundamentals

Eindhoven University of Technology

This work was supervised by:

Prof.dr.ir. J.D. Janssen

Dr.ir. C.W.J. Oomens

To Anne-Marie

Contents

Samenvatting

Het bepalen van de mechanische eigenschappen van biologisch materiaal met methoden, die zijn gebaseerd op homogene rekvelden (zoals trek-, afschuif- en torsieproeven) is lastig. Hoge stijfheidsverhoudingen door de aanwezigheid van vezels in het materiaal, gecombineerd met inhomogene eigenschappen, geven aanleiding tot niet uniforme spannings- en rekverdelingen. Daarnaast wordt het aantal mogelijke *in-vivo* proeven beperkt doordat kleine proefstukken moeten worden gemaakt, waardoor ook de interne structuur van het materiaal kan worden beschadigd.

Hendriks heeft een methode ontwikkeld, die geschikt is voor inhomogene rekvelden. Met die methode kunnen lokale materiaal eigenschappen worden bepaald, zelfs als deze inhomogeen over het materiaal verdeeld zijn. De drie elementen, waaruit de methode is opgebouwd, zijn: het gebruik van digitale beeldtechnieken om rekvelden te meten op proefstukken met arbitraire geometrie en belastingsgeval, de modelvorming van datzelfde proefstuk binnen de eindige elementen methode, en een parameter schattingsalgoritme op basis van minimum covariantie, waarmee numerieke en experimentele data kunnen worden gefit. Vergeleken met de traditionele wijze van materiaal beproeven, levert de methode extra vrijheid, die kan worden benut om de experimentele configuratie te optimaliseren.

Het doel van het onderzoek is een passende opstelling te vinden voor membranen met orthotrope eigenschappen en met hoge stijfheidsverhoudingen. Met passend wordt hier bedoeld: snelle convergentie van de te schatten parameters, de verschillen tussen gemeten en berekende verplaatsingen naderen de meetfout, en alle relevante parameters kunnen uit één enkel experiment bepaald worden. Dit wordt bereikt door systematisch de invloed van een gebruikt rekveld op de resultaten van het parameter schatten te bestuderen, zowel met behulp van simulaties als met echte experimenten. In de simulaties worden numerieke modelberekeningen verstoord met ruis en vervolgens beschouwd als "experimenten". Een groot aantal mogelijke experimentele configuraties zijn op deze wijze geanalyseerd en beoordeeld op bovenstaande criteria. Hierna zijn enkele significante gevallen daadwerkelijk uitgevoerd. De conclusies van dit onderzoek zijn:

- Voor orthotrope materialen met hoge stijfheidsverhouding heeft het opgelegde rekveld grote invloed op het schattingsgedrag. Voor isotrope materialen is dit niet het geval.
- Parameter bepaling op basis van uniforme rekvelden leidt tot slechte resultaten bij anisotrope materialen.
- In experimenten treden een aantal problemen op, die niet blijken uit de simulaties.

8

Summary

Mechanical testing based on uniform strain fields, like uniaxial, shear and torsion tests becomes very difficult when biological material is regarded. High anisotropic ratios due to fiber reinforcement and inhomogeneous properties tend to lead to nonuniform stress and strain distributions. Moreover, the need to extract small specimens limits the number of possible *in-vivo* tests and has the disadvantage that the tissue integrity will be disturbed.

Hendriks developed a numerical/experimental testing method, that is suitable for nonuniform strain fields. The method allows a local material characterization, even when the material has inhomogeneous properties. This approach combines three basic elements: measurement of strain distributions by means of a digital imaging technique on objects with arbitrary geometry and loading condition, finite element modeling of that object with the same geometry and loading and a minimum variance parameter estimation scheme to iteratively fit numerical on experimental data. Taking into account the extra freedom, compared to "traditional" testing, the method gives room for optimization of the experimental set-up.

The presented study aims at finding a suitable testing configuration for membranes with orthotropic properties and high stiffness ratios. Suitable means: fast convergence of the estimated parameters, residual deflections of the model and experimental output near the measurement error and the ability to estimate all relevant parameters from one experiment. This is done by systematically studying the nature of applied strain fields on the results of parameter estimation, using simulations and experiments. For the simulations numerical model calculations, disturbed with random noise, were used as "experiments". A large number of possible test set-ups were studied in this way and evaluated with regard to the above mentioned criteria. After that some of the most significant set-ups were used in real experiments to find out whether or not this would lead to the same results with regard to the estimation process. This led to the following conclusions:

- The kind of strain field that is used in an experimental set-up has a large influence on the results for orthotropic materials with high stiffness ratio and hardly any influence for isotropic materials.
- Uniform strain fields lead to poor results for anisotropic materials.
- A number of problems arise in experiments that cannot be simulated.

Notation

a	scalar
$\underset{\sim}{a}$	column
A	matrix
I	unit matrix
A^{-1}	inverse of A
A^{T}	transpose of A
$E\{A\}$	expected value of A
$[A_{11},..,A_{nn}]$	n × n diagonal matrix A

1

Introduction

The introduction of a range of new complex materials in mechanical engineering during the last decades has made the characterization of solids more than ever a problem of both numerical and experimental nature. The application of traditional ways of testing to these new materials causes a number of difficulties, which will make clear the motive of the present research.

1.1 CHARACTERIZATION OF SOLIDS

Mechanical properties of materials can vary with position. For instance in biological tissue, material properties such as orthotropic elasticity depend on the anatomical site of the sample. Technical materials like reinforced composites also may have - what we define - "inhomogeneous" properties. In the present study the concept of inhomogeneity refers to a scale where, for instance, the different orientation of the alignment of fibers in a material sample can be globally described.

Traditional methods for a quantitative determination of material parameters make use of specimens with well determined shapes which are assumed to be representative for the mechanical properties of the material. The design of a specimen and the selection of the applied load must lead to a homogeneous strain distribution in the central part of the sample. Measured displacements in this area can then be used to calculate the strain. Based on the hypothesis of a likewise homogeneous stress distribution, the stress in the central region is determined by equilibrium considerations.

However, the development of constitutive theories for the above complex materials requires a re-examination of traditional testing. Because these materials have inhomogeneous properties, homogeneous strains cannot be obtained; the manufacturing of specimens is hard or sometimes impossible and by disrupting the structure the specimen is often no longer representative for the behavior of the material in a undisturbed structure. Since St. Venants principle is not valid flaws due to clamping effects occur. The latter is particularly true for orthotropic materials with high stiffness ratio. Peters(1987) demonstrated that special care must be taken to assure that the desired information is obtained for biological materials. The outcome of this research calls for a generalization of the traditional approach to the characterization of complex materials.

1.2 THE IDENTIFICATION METHOD

A new numerical/experimental method for the characterization of biological tissues and composites, which considerably extends the scope that is covered by traditional methods, was presented by Hendriks(1991). Basic premises of this method are:

- The problem is to quantitatively determine the material parameters in constitutive equations. These constitutive relations are available in some mathematical form and give a reasonable description of the behavior of the material under consideration.
- Boundary value problems, concerning the materials of which parameters must be determined, can be solved accurately by means of an efficient computational algorithm.

Based on these premises Hendriks proposed a method that no longer demands the strain field to be homogeneous in some part of the loaded specimen. In this method more freedom is created for the design of experiments. More than homogeneous strain fields, we expect inhomogeneous strain fields to contain essential information about the material behavior. These facts offer new possibilities for the characterization of complex materials. Three new problems arise applying this method:

- The inhomogeneous strain distribution has to be measured. To fully utilize the freedom in experiments, loads must be applied in a more general way than in traditional testing.
- The resulting complex experimental set-up can only be analysed numerically.
- Numerical analysis and experiments must lead to determination of material parameters. Breaking the characterization down in a numerical and experimental part, a method has to be developed to confront experimental and numerical data.

Introducing the so-called *identification method* Hendriks brought up a solution for the above three problems. First inhomogeneous strain fields are measured optically using a grid method. A random dot pattern of markers placed on the sample's surface before and after deformation enable a contactless measurement of displacements and strains. The analysis of an experiment is performed by the Finite Element Method. Since numerical analysis can only be executed for a given set of (unknown) parameters, initial values must be available. Better estimates can be obtained using numerical and experimental data in a sequential minimum variance estimation algorithm.

The identification method was tested for a textile material. The example shows that the identification method can be applied succesfully. More attention must be addressed to the specific performance of this method, particularly regarding the experimental aspects (Hendriks, 1991).

1.3 INHOMOGENEOUS STRAIN FIELDS: THE OBJECTIVE

To explain the objective of the present research let us enlarge upon the importance of inhomogeneous strain fields. When using traditional methods the strain field has to be homogeneous in some part of the loaded sample under consideration. If the identification approach is applied, we wish the strain field to be inhomogeneous. There are two arguments for this:

- It can be expected that an inhomogeneous strain field contains more information about the material properties than a homogeneous strain field does.
- The extra freedom in the experimental set-up allows for the design of more suitable tests concerning the material.

This opens the way to a more effective determination of properties than is possible with traditional tests. However, the experimental freedom accustomed to the identification method also means the loss of a traditional protocol for the design and performance of experiments. Since the strain field is characteristic for a certain experiment and strain data are available at a very early stage of the characterization, it may well be possible that demands can be derived on the effectiveness of a model, regarding the determination of material parameters. If so, a new "protocol" based on strain distributions can be developed.

This basic idea, recommended by Hendriks, is the objective of the present study: by studying orthotropic materials with large stiffness ratios, the influence of experimental options like specimen geometry, applied load and boundary conditions on parameter estimation is investigated. Inhomogeneous strain distributions will play a major role in the judgement of experimental data.

1.4 METHOD AND OVERVIEW

To achieve the objective described in section 1.3, we will carry out an experimental quantitative characterization of materials in membrane structures and thin plates. This study will partly be done by means of numerical simulations, partly by means of experiments. A large number of numerical simulations are performed to find out what kind of strain field is suitable (and what kind is *not* suitable) for the determination of material parameters of isotropic and orthotropic materials. Specimen geometries, boundary conditions and the observational errors are chosen compatible with real experiments. To show that the suppositions from the simulations are correct a few outstanding simulations are repeated in real experiments. The experiments focus on the characterization of highly anisotropic materials as well as trying out the conclusions of the simulations.

Chapter 2 deals in more detail with the identification method according to Hendriks, chapter 3 presents the outcome of the numerical simulations and chapter 4 those of the experiments. In chapter 5 results will be discussed and in addition conclusions of the present research and recommendations for the future are given.

2

The identification method according to Hendriks

In this chapter the three elements of the identification method, mentioned in the introduction are described in short. These are the measurement of inhomogeneous strain fields, the finite element modeling of the experiment and the material parameter estimation. What follows is a short summary of the method as described by Hendriks(1991).

2.1 IDENTIFICATION METHOD

Based on the premises described in the introduction, Hendriks proposed a numerical/experimental technique for the characterization of the material behavior of solids: the identification method. This method is vizualized in figure 2.1.
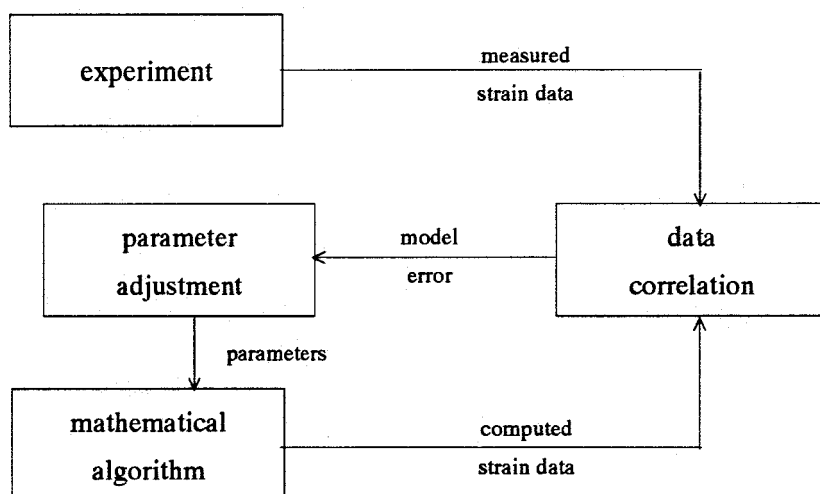

Figure 2.1: diagram for the identification method

In a common experimental situation the identification method aims at the measurement of strain fields. The position of a large number of markers, attached to the surface of the specimen is measured with a digital image technique, which will be discussed in more detail in section 4.2.3. The disadvantage of this optical method is that it is only possible to measure displacements on the outer surface of the specimen. Therefore strain field measurement is only relevant when the surface strain field contains enough information for a sufficient characterization of the whole specimen. This way the method is restricted to plate- or shell-like objects and membranes.

The analysis of a the experimental set-up can only be performed numerically. For this a standard finite element code is used, which enables varied model facilities. Numerical output is calculated using DIANA software (Borst *et al.*, 1985). The Finite Element calculations can only be carried out for a given set of (unknown) material parameters. Thus initial values must be available. Two different strategies can be applied to model the experimental set-up. The choise between the so-called "local" and "global" approach has a large influence on the way material parameters are estimated as will be discussed in section 2.3.

An iterative procedure is employed to determine material parameters. When the actual (inhomogeneous) strain distribution is measured and the model strain distribution is calculated as a function of the values of the parameters, the weighted difference is used for further adjustment of the parameters. This will be the subject in section 2.2.

2.2 PARAMETER ESTIMATION

The comparison between experimental data (measured displacements and forces) and the outcome of the finite element model must lead to quantitative values of material parameters. For this a sequential minimum variance estimator has been derived as summarized in the following mathematical equations (Hendriks, 1991);

$$\hat{\underline{x}}_{k+1} = \hat{\underline{x}}_{k} + K_{k+1} (\underline{y}_{k+1} - \underline{h}_{k+1}(\hat{\underline{x}}_{k})) \tag{2.1}$$

$$K_{k+1} = (P_{k} + Q_{k}) H^{T}_{k+1} (R_{k+1} + H_{k+1} (P_{k} + Q_{k}) H^{T}_{k+1})^{-1} \tag{2.2}$$

$$P_{k+1} = (I - K_{k+1}H_{k+1})(P_{k} + Q_{k})(I - K_{k+1}H_{k+1})^{T} + K_{k+1}R_{k+1}K^{T}_{k+1} \tag{2.3}$$

For nonlinear problems the material parameters, represented by a finite set of quantities $\underline{x}_{i}$, $i = 1...n$ are updated in equation (2.1). Column $\underline{y}_{k+1} = (y_{1},...y_{m})^{T}_{k+1}$ contains displacements components of material points (markers), where k is the ordering variable for the observations. Because non linear function $\underline{h}_{k+1}(x_{k})$ symbolizes the finite element calculation with last parameter values, adjustment is based on the difference between newly calculated and new experimental data, the residual, multiplied by the updated gain matrix K_{k+1}. This matrix is given by equation (2.2).

16

Although equation (2.2) may not be as easily comprehended as (2.1), the gain matrix comes about naturally looking at the different matrices involved. Bringing in the model's influence on parameter adjustment, matrix H_{k+1} defined as:

$$H_{k+1} = \left(\frac{\partial \underline{h}_{k+1}(\underline{x})}{\partial \underline{x}} \right)_{\underline{x} = \hat{\underline{x}}_k}$$

(2.4)

expresses the sensitivity of model output for parameter variations. To restrict the model's influence when parameter errors are large, the sum of squares is weighed with matrices P_k and Q_k. In a sequential minimum variance estimator matrix P_k represents the covariance of the estimate $\hat{\underline{x}}_k$ and is given by :

$$P_k = E\{(\hat{\underline{x}}_k - E\{\hat{\underline{x}}_k\})(\hat{\underline{x}}_k - E\{\hat{\underline{x}}_k\})^T\}$$

(2.5)

In practice Q_k prevents that the parameter error covariance P_k becomes to small. The matrix P_k is updated in a special way by equation (2.3). It can be shown that in a linear case this will lead to an optimal or truly minimum variance estimator (best linear unbiased estimator).

The quality of the observations is expressed by the measurement error covariance matrix R_k. By setting the matrix R_k the confidence in each seperate displacement measurement can be indicated, so that more accurate measurements dominate the gain matrix. This tends to lead to faster convergence of material parameters.

The estimator (2.1) to (2.3) is implemented as an extra module PAREST in the finite element code DIANA used for finite element modeling (Courage, Hendriks, 1989).

Note that to start the estimation of parameters not only initial guesses have to be available, but also the confidence in them must be expressed. Moreover an indication of the measuring error (distribution) is demanded.

2.3 GLOBAL APPROACH VERSUS LOCAL APPROACH

The techniques used for measuring the geometry of specimens of biological (but also technical) materials are poor, due to the complexity of the geometries involved and due to the fact that they easily deform under the external load. Although it may not be in all cases accurate enough, a satisfactory solution would be to place additional markers on the edge of the specimen surface to measure the specimen geometry. The boundary conditions for clamped edges are hard to model. Fibers in the material may cause that only a part of the clamped edge is loaded. Slip in the clamps will also introduce inaccuracies in the modeling of the clamped edges.

Modeling only a part of the specimen can be a possible solution for these problems. This "local approach" (Hendriks *et al.*, 1991) uses a selected set of markers to define the edges of the part of

the specimen under consideration (figure 2.2). Advantage of this approach is that the geometry of the model is relatively well defined. The displacements of the edge markers are used as boundary conditions for the element model. As a consequence it may be clear that forces cannot be part of the boundary conditions and thus stiffness parameters cannot be determined. Still it is possible to estimate the ratios between the different stiffness parameters.

Since modeling errors due to geometry and boundary condition errors do not occur in simulations a "global" approach is practiced in the following chapter, 3. Finally the "local" approach is used in case of the real experiments in chapter 4.
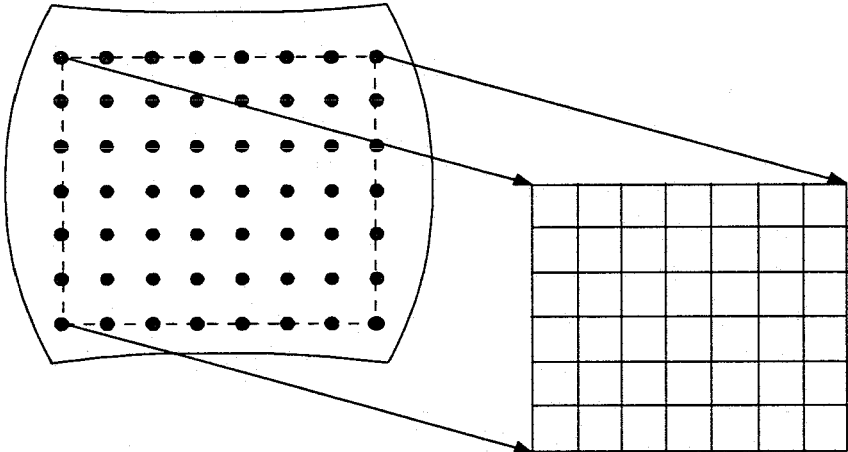
Figure 2.2: finite element model (right) for a part of the sample (left)

3

Parameter estimation for (an)isotropic elastic materials: simulations

3.1 INTRODUCTION

The numerical simulations described in this chapter performed for two basic reasons:

- Testing the identification method for isotropic materials and orthotropic materials with high stiffness ratio.
- Investigation of specimen geometry and boundary condition about the effectiveness of the model with regard to the determination of material parameters. In the present study this will be referred to as "identifiability" of the model (despite of different definitions of this word in the field of systems identification).

The variation of specimen geometry and boundary conditions brings about many different cases to be analysed. A systematic way to study these cases is to generate different sets of data, based on known material parameters. The calculated displacements in each set are disturbed by random noise. The application of the identification method results in the estimation of the original material parameters from the disturbed data. The outcome of these simulations is used to evaluate the different set-ups and will eventually lead to a set-up that is best suited for material characterization. The numerical experiments are restricted to those cases which actually can be performed in real experiments. This means that geometries and boundary conditions used in the simulations are chosen relatively simple.

In section 3.3 and 3.4 the identification results of respectively isotropic and orthotropic material will be presented. Before this the material behavior, the models and some validation tests are discussed in the section 3.2 PROCEDURE. Finally, conclusions referring to the outcome of this chapter are summarized in the section 3.5.

3.2 PROCEDURE

- The cases under observation are limited to membrane structures or thin plates. In that case it is necessary to account for possible wrinkling of membranes when negative in-plane stresses occur (Roddeman, 1987). The membrane elements used in the simulations do not have this ability, so wrinkling has to be avoided. In practice this means that large negative strains are avoided by choosing simple geometries (oblong, square, trapezium) and specific boundary conditions (tensile tests in one direction and biaxial tests).

- The material behavior is assumed to be orthotropic, linear elastic. Futhermore the material is supposed to have homogeneous properties; under plane stress conditions this means that the strain-stress relations are given by:

$$\begin{pmatrix} \varepsilon_x \\ \varepsilon_y \\ \gamma_{xy} \end{pmatrix} = T^T S T \begin{pmatrix} \sigma_x \\ \sigma_y \\ \tau_{xy} \end{pmatrix} \qquad (3.1)$$

$$\text{where} \quad T = \begin{pmatrix} \cos^2\alpha & \sin^2\alpha & 2\sin\alpha\cos\alpha \\ \sin^2\alpha & \cos^2\alpha & -2\sin\alpha\cos\alpha \\ -\sin\alpha\cos\alpha & \sin\alpha\cos\alpha & 2\cos^2\alpha-1 \end{pmatrix} ; \quad S = \begin{pmatrix} 1/E_1 & -v_{12}/E_1 & 0 \\ -v_{12}/E_1 & 1/E_2 & 0 \\ 0 & 0 & 1/G_{12} \end{pmatrix}$$

ε_x, ε_y and γ_{xy} are the linear strain components in an arbitrary coordinate system (x,y,z), while σ_x, σ_y and τ_{xy} are the Cauchy stress components. Compliance matrix S contains 4 independent material parameters: Young's moduli E_1 and E_2, Poisson's ratio v_{12} and shear modulus G_{12}. Transformation from the model coordinate system to a coordinate system that matches the axes of symmetry of the material is represented by matrix T, in which α is the angle from the arbitrary model x-axis to the material 1-axis. Thus the material's quantitative behavior can be described by 5 parameters:

$$x^T = (E_1, E_2, v_{12}, G_{12}, tg(\alpha)) \qquad (3.2)$$

For isotropic behavior, E_1 equals E_2 (=E), v_{12} becomes v, $G_{12}=E/2(1+v)$ and α is not defined. In that case 2 parameters E and v remain.

- The numerical experiments and the determination of parameters are executed using finite element code DIANA. The models consist of 4-noded plane stress elements (4 integration points) The simulated displacement data are calculated using kinematic boundary conditions i.e. nodes on one or more edges are forced to translate; the resulting reaction forces in these nodes are applied when the material parameters are determined (global approach).

- Based on the above remarks, we distinguish four basic features: material behavior, specimen geometry, boundary condition and orthotropic orientation. The latter, characterized by tg(α), is merely a kinematic parameter but can also be seen as an experimental parameter for experiments with orthotropic material. For each feature several alternatives are proposed in figure 3.1. Each combination of alternatives leads to a different numerical experiment.

- In Norton (1986) several tests to judge the identification of models are suggested. Here the following test are used to evaluate the performance of the models and the effect of the identification method in general:

  - The displacements y_k before estimation of parameters; looking at plots of strain fields and principle strain domains is recommended (see sections 3.3.1 and 3.4.1).
  - The parameter estimates x_k in the light of background knowledge.
  - The fit of the model to the measurements by means of the residuals $y_k - h_k(\hat{x}_N)$ at the final iteration N.
  - The estimated covariance of the estimation errors P_N.
  - The behavior of the model as a whole. A model's prediction of measurements other than used to estimate the parameters may reveal poor performance of the model. The vality of the model can be expressed for instance by the mean square of residuals:

$$s^2 = \frac{1}{mN} \sum_{k=1}^{N} (y_k - h_k(\hat{x}))^T (y_k - h_k(\hat{x})) \tag{3.3}$$

where m is the dimension of the new measurements $y_1 ... y_N$.

Depending on which case is studied, one or the other test may detect a poor performance of the model. Unfortunately, it is hard to predict the best technique in a particular case. When simulated measurements are considered, more tests can be added:

- The convergence of parameter estimates to the original values.
- Estimation of the covariance of the estimation error P against the real estimation error based on real and estimated parameters.
- The convergence of the mean square of residuals to the theoretical expectation of the mean square error (no model errors):

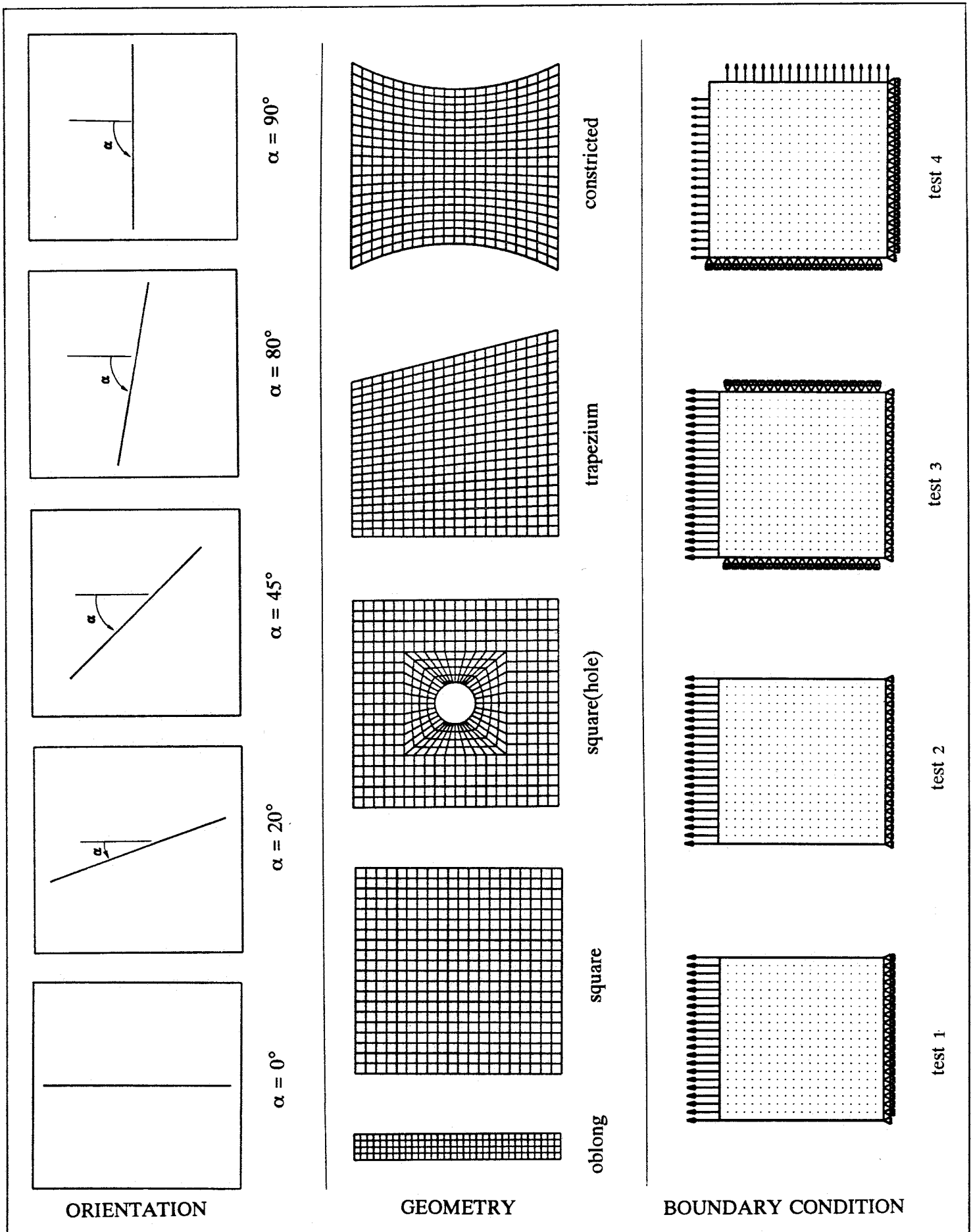$$E(s^2) = \frac{1}{mN} \sum_{k=1}^{N} tr(R_k) \tag{3.4}$$

Figure 3.1: finite element models

The next sections will present simulation results for the cases proposed in figure 3.1. The results are divided essentially in two parts. The first half (section 3.3) covers the simulations with isotropic models, the remainder of the results however, concerns the identification of orthotropic materials with stiffness ratio 1 : 10 (section 3.4).

3.3 ISOTROPIC RESULTS

The identification of isotropic materials aims at the determination of 2 parameters, *i.e.* Youngs modulus E and Poisson's ratio v. The used isotropic models feature (orientation of material symmetry axes is undefined):

- 5 different geometries
- 5 different sets of boundary conditions

It may be clear that presenting the results of all possible alternatives is difficult to do. Therefore the results of two main groups are discussed. These groups are:

- geometry variation for a simple uniaxial tensile test (test 1).
- boundary condition variation for oblong and square geometries.

The simulated measurements are based on the nondimensional parameters:

$$E = 0.5 \ ; \quad v = 0.2 \tag{3.5}$$

and are disturbed with a random error by adding a realization of a zero mean normal distribution. The standard deviation of the noise is 10^{-3}, based on accuracy measurements under optimal conditions in real experiments (maximum dimension of the specimen is 100). Before the simulated data are used for the estimation of parameters, we will discuss the strain fields and displacement fields of perfect observations.

3.3.1 STRAIN FIELDS

Isotropic modeling of material with homogeneous properties mostly yields homogeneous strain and displacement fields in large parts of the specimen. In fact this is confirmed by all isotropic models in these simulations (figure 3.2). In the principle strain domain (principle strain ε_1 versus ε_2 for all measured material points) homogeneity of a strain field is represented by a group of dots close together. The position of the group's centre gives information about the positive/negative strain ratio. The group turns into one point when a ideal homogeneous strain distribution is approximated (this is the case for test 1).

Restricting the experiment in any way often leads to expansion of the dot pattern and/or a

translation of its centre. This is particularly true for another extreme case when contraction of the specimen is totally restricted in ε_2-direction (test 3); since only strains in one direction are tolerated, dots can only be found on the principle strain ε_1-axis. Test 2 shows the expected pattern in a case that lies between the extremes 1 and 3.
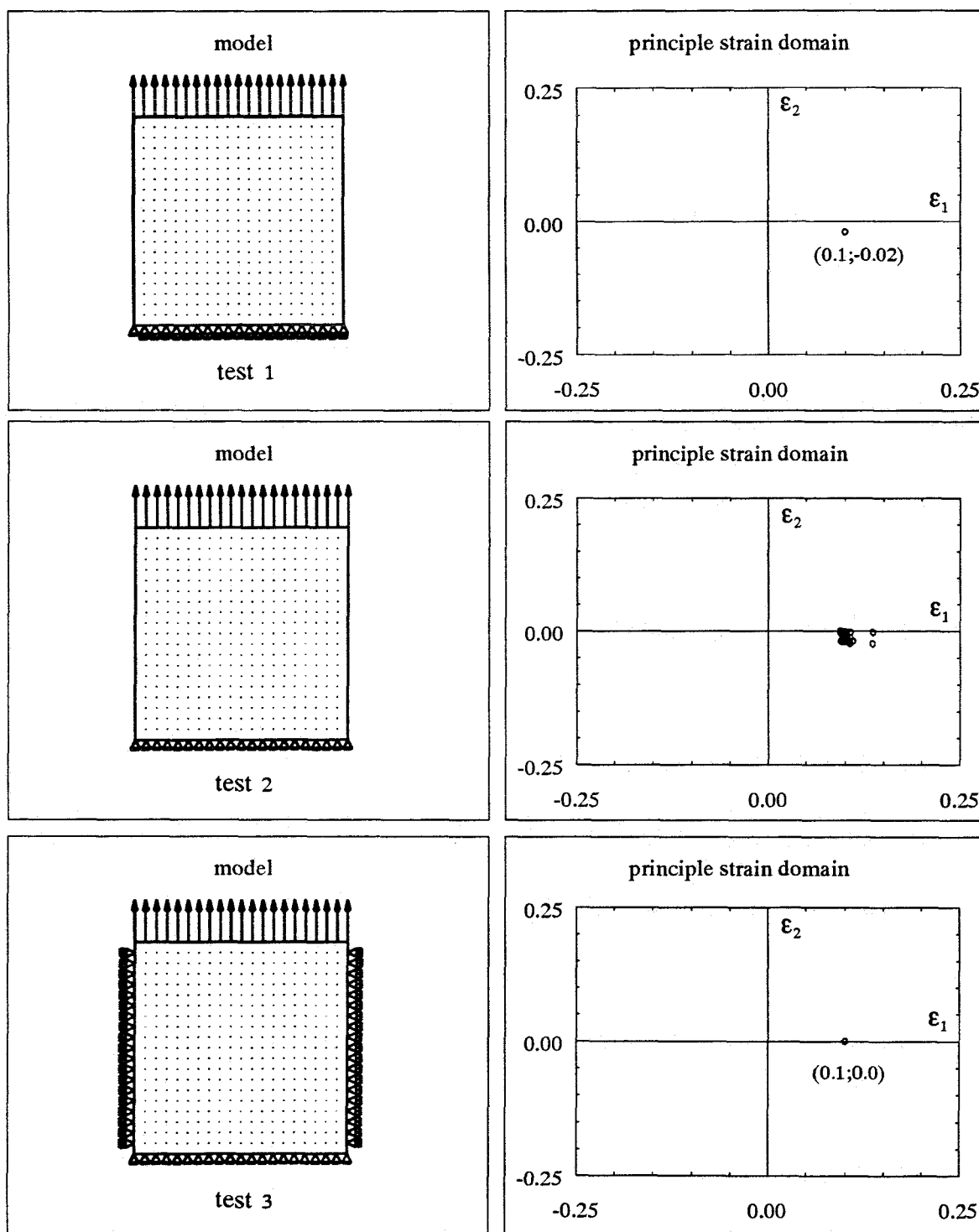
Figure 3.2: plots of the principal strain domain; a homogeneous strain field is characterized by a single point in the strain domain.

When stresses are geometrically forced to distribute in a inhomogeneous way through the specimen, strains will come forward inhomogeneously as a result. This is practiced in the simulations with specimens of trapezium geometry, constricted geometry and square geometry with a modeled hole (figure 3.3).
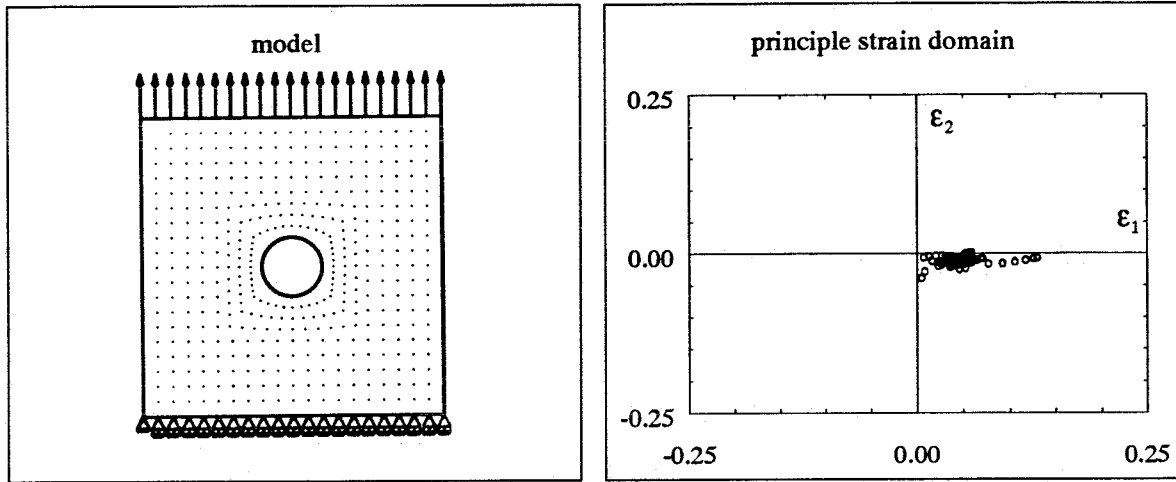
Figure 3.3: inhomogeneous strains plotted in the principle strain domain

3.3.2 PARAMETER ESTIMATION

To initiate the recursive parameter estimator an initial guess $\hat{x}_0$ for the parameter values and an initial guess for the error covariance of $\hat{x}_0$ are needed. We consider P_0 diagonal and the elements correspond with the squared errors in the initial guess. In table 3.1 the values for $\hat{x}_0$ and P_0 used in all simulations are given.

The diagonal elements of covariance of measured displacements R_1 is set to 10^{-6}. Furthermore we will take Q diagonal with $Q = \lceil 10^{-3}, 10^{-3} \rfloor$ for convergence reasons.

Parameter estimation comprises 5 iterations.

An evaluation of the identification results for isotropic models with different geometry is presented in tabel 3.2. This tabel contains norms for the displacement field residual and the material parameters. Furthermore, the global convergence is evaluated with "gain norm", defined as $\| K_{k+1}(y_{k+1} - h_{k+1}(x_k)) \| / \| (y_{k+1} - h_{k+1}(x_k)) \|$ (see equation (2.1)).

For all cases the parameters converge in the same manner to the original values (figure 3.4a); the residual is randomly distributed and reaches a minimum at 10^{-3} (standard deviation, 3.4b). The estimated error in the parameters shows a good agreement with the expected parameter error when parameters are converged ($\sqrt{(P_5)}_{11} \approx 1.10^{-5}$ and $\sqrt{(P_5)}_{22} \approx 1.10^{-4}$).

Tabel 3.1: original values and initial guesses for the material parameters

isotropic parameters x_i	original value x_i	initial guess x_0	$\sqrt{(P_0)_{ii}}$
x_1	0.5	0.25	0.25
x_2	0.2	0.35	0.1

orthotropic parameters x_i	original value x_i	initial guess x_0	$\sqrt{(P_0)_{ii}}$
x_1	0.1	0.25	0.25
x_2	1.0	0.35	0.15
x_3	0.2	0.35	0.15
x_4	0.5	0.35	0.15
x_5	$0.0/0.36/1.0/5.7/\infty$	...	0.15

The results for the identification of oblong and square specimens under different testing conditions are evaluated once more in tabel 3.2. Good performances are given by simple tensile tests, where loading occured in one direction (test 1) and the biaxial tests (4). Deviations in estimated and expected parameter values are obvious in case of restricted experiments; these experiments lack information about contraction of the specimen, as a result Poisson's ratio is badly estimated.
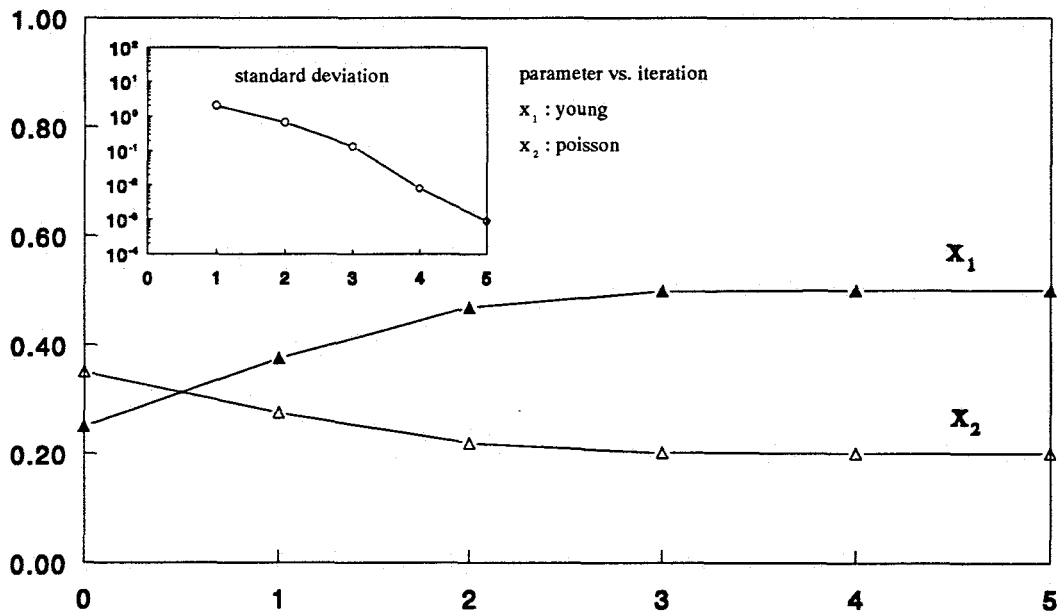

Figure 3.4: estimation results: (a) parameter vs. iteration, inside (b) standard deviation of the residual of the displacement field.

A remarkable difference is noticed between square and oblong models, loaded according to test 2: because the number of nodes inside the square element mesh is bigger than inside the oblong mesh, more markers are situated inside the contraction zone. This way more information is available about the parameter v leading eventually to a much better estimate. In a real experiment where the number of markers can be the same in both experiments, still better results may be expected for the square geometry. Because of boundary conditions, the square specimen has a larger inhomogeneous strain area than the oblong specimen. Thus the strain field for the square specimen contains more information .

Tabel 3.2: evaluation isotropic results

Model	Standard Deviation residual/meas.error	Parameters E/E_{real}	v/v_{real}	Gain Norm (10^{-4})	Identification
TEST 1					
oblong	0.91	1.00	1.00	7.01	+
square	0.98	1.00	1.00	3.29	+
sqr.(hole)	4.64	1.00	1.00	0.66	+
trapezium	1.00	1.00	1.00	3.23	+
constr.	1.00	1.00	1.00	3.23	+
OBLONG					
test 1	0.91	1.00	1.00	7.01	+
test 2	44.3	1.00	0.51	0.13	-
test 3	1.73	0.79	2.45	325.	-
SQUARE					
test 1	0.98	1.00	1.00	3.29	+
test 2	1.00	1.00	1.00	3.06	+
test 3	7.88	0.79	2.45	32.2	-
test 4	1.01	1.00	1.00	3.38	+

3.3.3 CONCLUSIONS

• On the whole isotropic models can be succesfully identified, regardless geometry and boundary condition influences. The material parameters are traced back from disturbed data to their original values and the final residual is reduced to the measuring error. The shown convergence course appears constant.

• Exceptions to the above are models on which experimental data lack information on contraction. A good example of this is a "confined" test, such as test 3. Looking at the principle strain domain may help detecting such model.

The next section is dedicated to orthotropic models.

3.4 ORTHOTROPIC RESULTS

In characterizing fiber composite material and biological tissue we must be sure to take into account orthotropic behavior with a high stiffness ratio. For these materials shear moduli and contraction coefficients are particularly hard to find by traditional testing. Therefore the identification method is tested with orthotropic models where:

$$E_1 : E_2 = 1 : 10 \tag{3.6}$$

The nondimensional values used for calculation of simulated data are:

$$
\begin{aligned}
E_1 &= 0.1 & ; & \quad E_2 &= 1.0 \\
v_{12} &= 0.2 & ; & \quad G_{12} &= 0.5
\end{aligned}
\tag{3.7}
$$

Note that for $\alpha = 0°$ tensile forces are applied in the stiffest direction of the specimen (figure 3.5). Marker (node) displacements are disturbed with similar errors as described in the section for isotropic models. Here the main subjects of investigation are the specimen geometry, boundary condition and the orientation of material symmetry axes.

Actual studies are performed on:

- square geometry specimens with $\alpha = 0°$, $20°$, $45°$, $80°$ and $90°$ in uniaxial tensile tests and biaxial tests (1 and 4).
- geometry variation for $\alpha = 45°$ direction in uniaxial and biaxial tests.
- variation of boundary condition (test 1,2,3 and 4) for square geometry specimens and $\alpha = 0°$ and $45°$ direction.
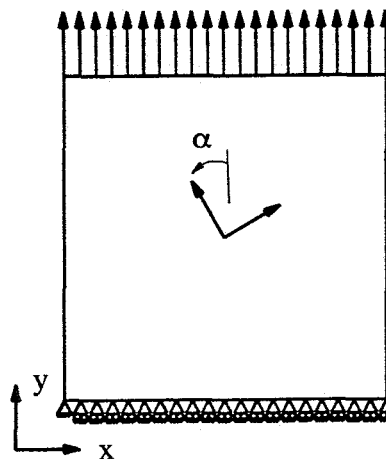

Figure 3.5: definition of rotational angle α

3.4.1 STRAIN FIELDS

The interpretation of strain fields of orthotropic models is less evident than in the case of isotropic models. Although similar trends can be observed when boundary condition and geometry are varied, pointing out typical features is more difficult. Homogeneous strain distributions appear only in a small number of cases, where loading occurs in one direction. The angle of material symmetry axes α however gives some room for discussion.

Figure 3.6 shows plots in the strain domain of a square geometry specimen under biaxial loading conditions. For each different angle α a different pattern can be seen. The patterns for $\alpha = 0°$, $80°$ and $90°$ resemble, supporting the fact that the contribution of the shear modulus to the deformations in these cases is relatively small (and constant) (Chamis, Sinclair, 1977). Small angles α (between $0°$ and $45°$) tend to lead to more inhomogeneous strain fields. Consequently the direction of material symmetry - compared to the angle of loading - comes forward as a strong experimental parameter.

3.4.2 PARAMETER ESTIMATION

The recursive parameter estimator is started with an initial guess $\hat{x}_0$ for the parameter values and an initial guess for the error covariance of $\hat{x}_0$. Like before, we consider P_0 diagonal, the elements corresponding with the squared errors in the initial guess. In table 3.1 the values for $\hat{x}_0$ and P_0 used in the simulations are given.

The diagonal elements of covariance of measured displacements R_i is set to 10^{-6}.

Estimation of parameters (3 iterations) is repeated 2 or 3 times (depending on convergence of parameters) adjusting initial parameters at each re-start. Matrix Q is take diagonal with $Q = \lceil 10^{-3}$, 10^{-3}, 10^{-3}, 10^{-3}, $10^{-3} \rfloor$ initially and adjusted during the second and third run for faster convergence.

First the results of α's variation are validated. We distinguish two finite element models: one features a square geometry in a simple uniaxial tensile test (test 1), the other features a biaxial test (4). Tabel 3.3 shows the evaluation of the final parameter estimates and convergence speed for the investigated angles α for both tests. Although we end up with convergence of material parameters in some cases, we have to disapprove the overall performance of the model loaded in only one direction; still the standard deviation of the residual (apart from obvious divergence for $\alpha = 20°$) is reduced. The performance of the biaxial model is much better; again for $\alpha = 20°$ divergence appears.

The results for variation of boundary conditions (tabel 3.4) show good performances for the biaxial and - more remarkable - the "confined" test (test 3), when $\alpha = 45°$. Still we find the model loaded in one direction and clamped along the lower edge (test 2) hard to identify. When the specimen is loaded in its stiffest direction ($\alpha = 0°$) material parameters are well estimated only in case of test 2 and 4. These results support the assumption that the biaxial test is superior. Moreover we conclude that the choise of rotational angle of material symmetry (with respect to the loading angle) has large influence on the identification of anisotropic models.
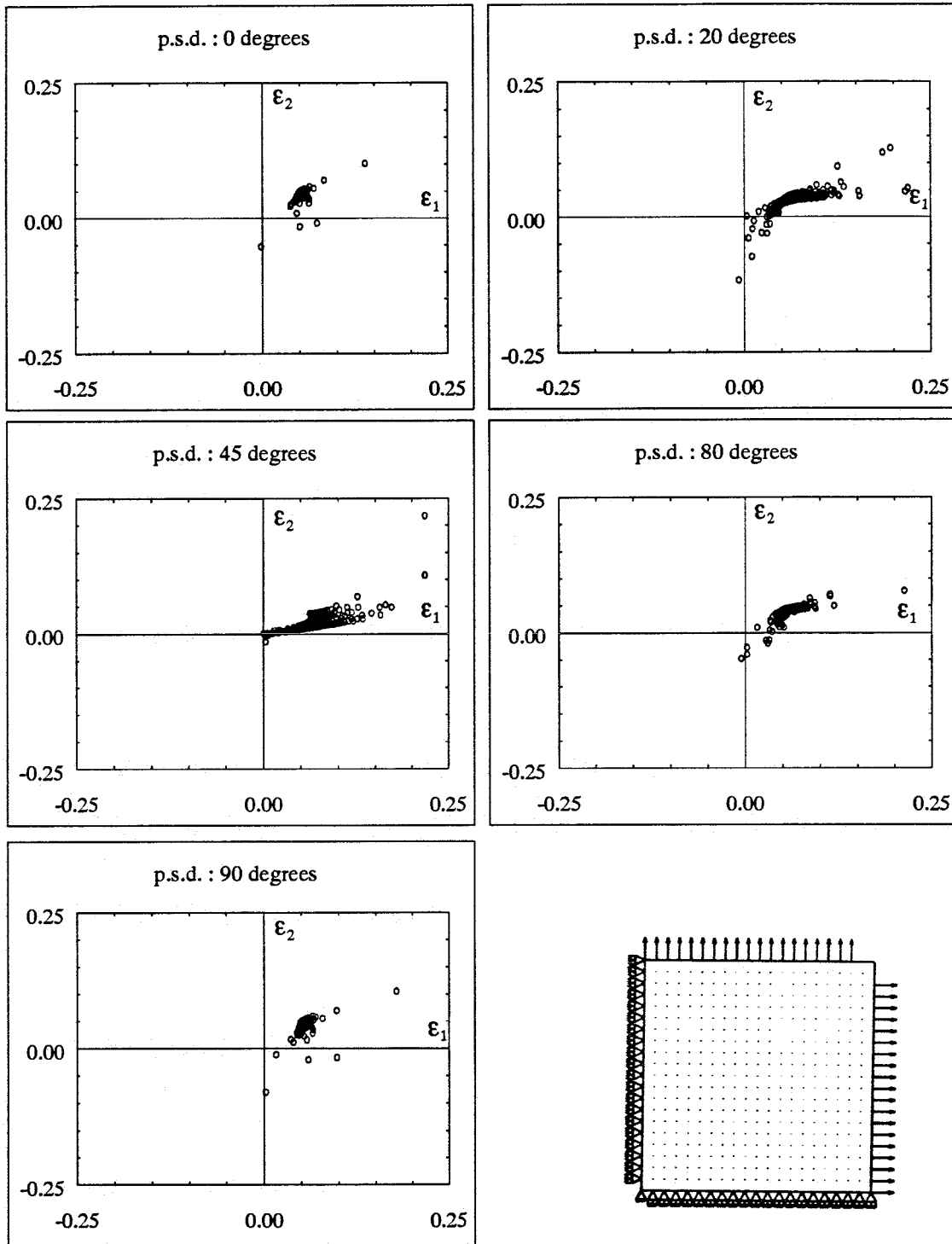
Figure 3.6: principle strain domain (p.s.d.) for α = *0°,20°,45°,80° and 90°*

Different geometries are tested in a biaxial and uniaxial model ($\alpha = 45°$). Tabel 3.5 shows that the overall performance (read: identifiablity) of these models is good; we found divergence for a trapezium geometry specimen loaded in a uniaxial tensile test.

Tabel 3.3: evaluation orthotropic results: variation of α

Model	S.D. r./m.e.	Parameters E_1/E_{1real}	E_2/E_{2real}	v_{12}/v_{12real}	G_{12}/G_{12real}	$tg(\alpha)/tg(\alpha)_{real}$	G.N. (10^{-3})	Identif
TEST 1								
$\alpha = 0°$	0.98	3.22	0.99	1.73	0.83	▲	1.42	-
$\alpha = 20°$	263.	4.71	0.91	0.05	17.7	2.90	35.3	-
$\alpha = 45°$	5.67	0.91	1.02	0.88	0.69	0.91	325.	-
$\alpha = 80°$	0.99	0.99	0.79	3.91	0.89	0.99	2.05	-
$\alpha = 90°$	0.98	1.00	0.70	0.75	0.58	▲	2.09	-
TEST 4								
$\alpha = 0°$	1.00	1.00	1.00	1.01	1.00	▲	0.02	+
$\alpha = 20°$	8837	0.38	1.00	0.05	0.55	0.51	1.37	-
$\alpha = 45°$	1.03	1.00	1.00	1.00	1.00	1.00	0.00	+
$\alpha = 80°$	1.00	1.00	1.00	1.00	1.00	1.00	0.22	+
$\alpha = 90°$	560.	0.99	1.00	0.96	0.99	▲	6.72	+

Tabel 3.4: evaluation orthotropic results: variation of boundary condition

Model	S.D. r./m.e.	Parameters E_1/E_{1real}	E_2/E_{2real}	v_{12}/v_{12real}	G_{12}/G_{12real}	$tg(\alpha)/tg(\alpha)_{real}$	G.N. (10^{-3})	Identif
$\alpha = 0°$								
test 1	0.98	3.22	0.99	1.73	0.83	▲	1.42	-
test 2	1.60	1.00	1.00	1.00	0.99	▲	628.	+
test 3	757.	6.02	0.55	2.45	0.45	▲	17.4	-
test 4	1.00	1.00	1.00	1.01	1.00	▲	0.02	+
$\alpha = 45°$								
test 1	5.67	0.91	1.02	0.88	0.69	0.91	325.	-
test 2	5363	1.00	0.42	0.05	0.22	0.14	15.7	-
test 3	1.18	1.00	1.00	0.99	1.00	1.00	62.6	+
test 4	1.03	1.00	1.00	1.00	1.00	1.00	0.00	+

Before closing off this section, some remarks have to be made about the convergence of material parameters. In some studied models one parameter, often $tg(\alpha)$, shows divergence when the initial guess is too far from the original value. As a consequence, other parameters are badly estimated also. In above simulations this means that this model more or less is rejected. Stricktly speaking this may be unfair for convergence is not excluded when initial conditions are chosen more appropriate. The basics of the simulations however, are such that each model gets equal chance when it comes to determination of material parameters.

Tabel 3.5: evaluation orthotropic results: variation of geometry

Model	S.D. r./m.e.	Parameters E_1/E_{1real}	E_2/E_{2real}	v_{12}/v_{12real}	G_{12}/G_{12real}	$tg(\alpha)/tg(\alpha)_{real}$	G.N. (10^{-3})	Identif
TEST 1								
oblong	0.95	0.72	0.83	1.53	0.41	0.73	5.65	-
square	5.67	0.91	1.02	0.88	0.69	0.91	325.	-
sq.(hole)	8.72	1.00	1.00	0.99	1.00	1.00	67.0	+
trapezium	9379	0.24	0.89	2.45	200.	-1.2	2.e4	-
TEST 4								
oblong	1.e4	0.35	3.24	0.05	1.03	1.31	0.00	-
square	1.03	1.00	1.00	1.00	1.00	1.00	0.00	+
sq.(hole)	4.68	1.00	1.00	1.00	1.01	1.00	1.00	+
trapezium	1.00	1.00	1.00	1.00	1.00	1.00	1.14	+

3.4.3 CONCLUSIONS

Identification of orthotropic materials depends on the model used:

• The rotational angle of material symmetry α is an important experimental parameter in the research of identifiability of orthotropic models with high stiffness ratio. Variation of α leads to strong pattern chances in the principle strain domain, which indicates a likewise influence of α on parameter estimation. Seen in this background the performance of the 20° off-axis test is rejected. Optimal angles α range from 45° up to 80°. For $\alpha = 45°$ good results are found even for "confined" testing.

• The simulations using favourable $\alpha = 45°$ as well as less favourable $\alpha = 0°$ prefer biaxial testing, where loading occured in two different directions. In general biaxial tests give better results than tests with loading in one direction.

• Under favourable testing conditions, the specimen geometry has relatively small influence on the identifiability of models.

3.5 SUMMARY AND GENERAL CONCLUSIONS

This chapter has adressed the problem of identification for isotropic and orthotropic materials. Numerical simulations of experiments were performed to investigate the influence of geometry, boundary condition and orientation of material symmetry axes on the determination of parameters. In the case of isotropic models calculations were based on 5 geometries and 4 different boundary conditions. The simulated data used to trace back the parameters were disturbed by a random error. Anisotropic simulations were performed for different orientations of material symmetry axes; data sets were collected for 0°, 20°, 45°, 80° and 90° off-axis tests. The influence of geometry and boundary condition was also studied.

32

The evaluation of the results can be summarized in the following general conclusions:

- For isotropic materials there is hardly any influence of the choise of experiment or strain field on the parameter estimation process. The principle strain domain gives sufficient information about identifiability of a model. In case of orthotropic materials with high stiffness ratio the choise of strain field has large influence on the estimation results.
- Uniform strain fields lead to poor results for anisotropic materials.
- Poor results were obtained in adaptions of the normal uniaxial tensile tests where loading occured in one direction, but with variations in the rotational angle of material symmetry and specimen geometry to obtain nonuniform strains.
- Very good results were found using biaxial models, where loading occured independently in two different directions. In these cases geometry appeared unimportant. It is recommended to choose the material symmetry angle different from the loading angle.

We must realize that the above conclusions are conclusions from simulations. To confirm these conclusions real experiments have to be done for some outstanding cases. These experiments will be the subject of chapter 4.

4

Parameter estimation for anisotropic elastic materials: experiments

This chapter deals with the determination of material parameters of anisotropic material by means of experiments. Several experiments previously performed as simulations are carried out on homogeneous membranes with orthotropic elastic properties.

4.1 INTRODUCTION

On the whole the numerical simulations of chapter 3 are merely an introduction to the experiments described in this chapter. Main reason for these experiments is to test the identification method for anisotropic elastic material with high stiffness ratio. The conclusions concerning the simulations are used in the discussion of the parameter estimation outcome. To prove the value of the numerical simulations not only experiments with (expected) optimal performance are carried out, but also some tests of which the performance at the end of chapter 3 was disapproved.

Section 4.2 describes the experimental set-up. This includes a description of the material, the selection of specimen geometries and boundary conditions based on the numerical simulations and a description of the strain distribution measurement and biaxial tensile testing apparatus. Section 4.3 includes the finite element modeling of a part of the specimen using the "local approach". Main issue of section 4.4 is the parameter estimation of four unknown parameters (ratio's and coefficients) in eight experiments; discussion of results and conclusions concerning the experiments are the subjects of section 4.5 and 4.6.

4.2 THE EXPERIMENTAL SET-UP

4.2.1 THE MATERIAL

Silicon rubber material is used for the experiments. Figure 4.1 shows the structure of the material. The pictured pattern on the material surface is applied in a regular sequence by local thickening.

The angle β between the "fibers" is 62°. On a scale, large enough to average local properties, the material can be regarded as homogeneous. Moreover, the specimens can be considered as membranes under plane stress conditions. Because of this structure, we assume an orthotropic model for the mechanical behavior with $\bar{e}_1$, $\bar{e}_2$ and $\bar{e}_3$ (seen in 4.1) as directions of symmetry to be appropriate. The stress-strain relations under plane stress conditions are given by eq.(3.1).
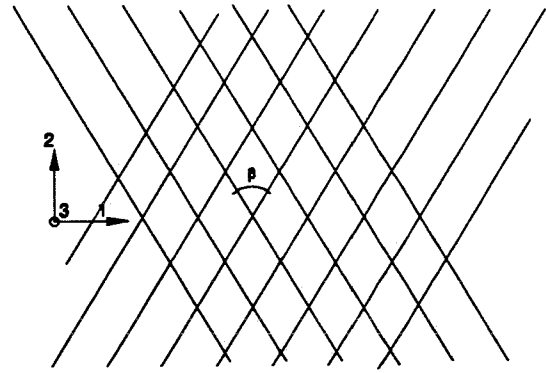
Figure 4.1: material structure

4.2.2 SPECIMEN CHOISE AND BOUNDARY CONDITION

Chapter 3 featured simulations on objects with different geometry, boundary conditions and angle of material symmetry. From all possible configurations nine experiments are selected. These are:

Tabel 4.1: experiments

	trapezium test 2 / α=45°		square (hole) test 2 / α=45°	
square specimen test 3 / α=45°				square specimen test 3 / α=0°
		square specimen test 2 / α=45°		
square specimen test 4 / α=45°				square specimen test 4 / α=0°
	square specimen test 2 / α=20°		square specimen test 2 / α=0°	

In our set-up we use membranes of 100 × 100 × 0.25 mm³. The experiments are performed on a biaxial tensile testing machine. The specimens are actually clamped over 100 mm and can be forced to stretch either in one or in two directions in the plane of the membrane. Although not neccessary - we use the "local" approach - forces are measured in the main ($=\bar{e}_2$) direction (from 3.76 N up to 19.2 N). To exclude visco-elastic effects, the material is relaxed 180 seconds before measuring the strains. The avarage strains are 0.02. Wrinkling of membranes is avoided as much as possible. The strain distribution and shape of the model is measured with markers on the surface. The next section describes the position measurement of markers.

4.2.3 STRAIN DISTRIBUTION MEASUREMENT

The positions of markers are measured with a video tracking system (Hentschel GmbH, Hannover) based on random access cameras. This system is developed in order to measure positions in space and time, but will be used here only to record seperately positions of markers in a reference and deformed situation.

A regular pattern of markers of retro-reflective foil on an illuminated surface leads to an identical pattern of bright points in the camera image. The tracking system uses this characteristic of reflective markers to identify the global positions during search-scanning. Everytime the system detects a marker a window is defined with its centroid at the centroid of the marker and with a size larger than the diameter of the marker. After all markers are found the system only scans windows, adjusting the window positions when markers undergo a displacement. During this window scan mode the exact position of the markers centroids are determined and written to personal computer memory.

Before measuring, the tracking system is set according to the experimental demands by choosing several system parameters. The setting used for the present experiments can be found in tabel 4.2. The actual influence of the listed parameters on *for instance* position accuracy is explained by Zamzow(1990) and Hendriks(1991). Also given in tabel 4.2 are the technical details on the experimental configuration and some information about the observation errors.

4.3 NUMERICAL MODELING

In section 2.3 two possible strategies are proposed to model experiments within the identification method. The approach which was practiced in the numerical simulations, introduced as "global approach", demands measurement of forces and boundary conditions to be able to model the experiment. In practice it is relative hard to measure quantities like the object geometry and loading direction. Because these play an important role in the modeling of the experiments, this is a disadvantage, leading to large and unpredictable model errors.

An alternative approach uses marker positions and displacements to model just a part of the specimen under loading conditions. This strategy leaves out forces and offers ways to model the geometry more accurate. However the "local" approach results in estimation of stiffness ratio's due to the fact that no actual information about the stress in the specimen is used.
As a consequent the following parameters will be estimated:

$$\underset{\sim}{x}^T = (\check{E}_1, \nu_{12}, \check{G}_{12}, tg(\alpha)) \tag{4.1}$$

where $\check{E}_1$ and $\check{G}_{12}$ denote a relative, nondimensional stiffness and shear modulus respectively:

<u>Measurement system</u>

Video tracking system	:	Hentschel Video interface 84.330
Camera body/amplifier	:	Hamamatsu C1181
Lens	:	Fuji photo optical 1:1.4/50
Field of view	:	20×20 cm^2
Calibration factor	:	166 pixels/mm

<u>System parameters</u>

Camera #	:	2
Window size	:	1.4 % of F.O.V.
# Markers	:	80
Sample rate	:	1875 Hz
Limits	:	left: 0, right: 4095
Step	:	5
Acquisition rate	:	1875 Hz
Sample rate/marker	:	23.4 Hz
# Samples/target	:	204.8
Acq. time	:	11.2 s
Maximum resolution	:	16384

<u>Accuracy</u>

Covariance of displacement components : 4.5 pixel^2

$$\check{E}_1 = E_1/E_2 \quad ; \qquad \check{G}_{12} = G_{12}/E_2 \tag{4.2}$$

and v_{12} represents the Poisson ratio as defined in section 3.2, while tg(α) denotes the positive rotation of the material axes.

Figure 4.2 shows one of the measured marker position fields next to the final finite element mesh used for parameter estimation. This 224-element mesh is generated with I-DEAS pre- and postprocessing software and is translated to DIANA for use as numerical model. Displacements of the inner 45 markers are calculated by interpolation of nodal displacements. Boundary conditions include the measured displacements of the edge nodes (all measures in pixels).
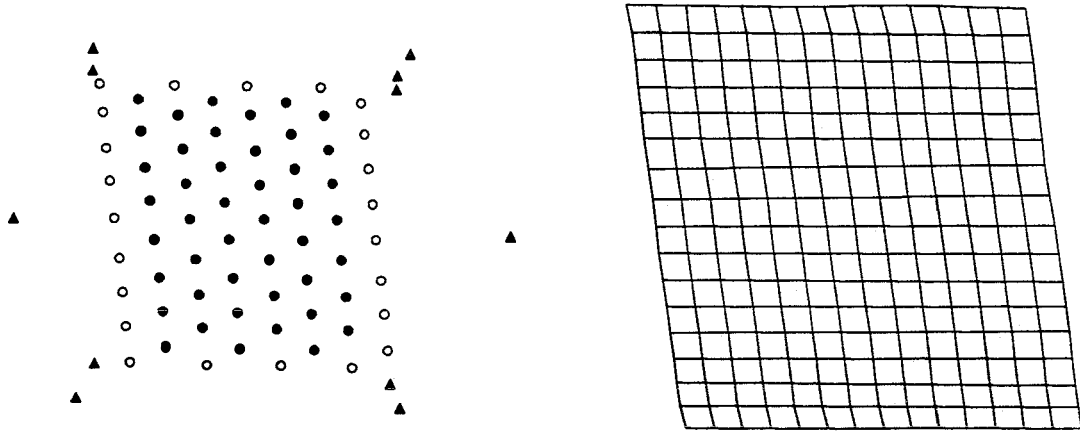
Figure 4.2: (left) measurement of the geometry of the specimen part: image coordinates of the observation markers (•), contour markers (○) and remaining markers (▲); (right) the finite element mesh

4.4 PARAMETER ESTIMATION

The recursive parameter estimator is started twice with initial guess:

$$\hat{x}_{0_1}^T = (0.1, 0.2, 0.1, 0.75), \quad \text{and} \quad \hat{x}_{0_2}^T = (0.5, 0.3, 0.5, 2.00) \tag{4.3}$$

The covariance of the parameters P_0 is considered diagonal and is set to $\lceil 10^{-1}, 10^{-1}, 10^{-1}, 10^{-1} \rfloor$. The diagonal elements of the covariance of measured displacements R_1 are each set to the actual square measuring error. Diagonal matrix Q is chosen rather arbitrary $\lceil 10^{-4}, 10^{-4}, 10^{-4}, 10^{-4} \rfloor$ and is adjusted in some cases to speed up convergence. The number of iterations is 16.

Figure 4.3 shows the estimates of the four material parameters as a function of the iteration counter, starting from both initial guesses. It can be observed that the parameters converge (the poisson ratio is limited to 0.4999). The matching experiment is characterized by a square specimen, the angle of material symmetry $\alpha = 45°$ and loaded under biaxial conditions (test 4). A similarly designed experiment worked very well in the numerical simulations. Because of this it is remarkable that the estimated value of $tg(\alpha) = 0.136$, $\alpha = 7.74°$ is far from what may be expected. The determined angle α possibly indicates the fiber direction more than the material symmetry orientation; in that case, considering the material structure, another solution of the identification problem (*i.e.* another minimal residual field) should be found symmetric to 45°. Figure 4.4 shows this is the case: calculating the standard deviation of the residual as function of α we see two minima, one at 7.7°, the second at 82.3°. The angle β between the fibers is estimated 74.5°.

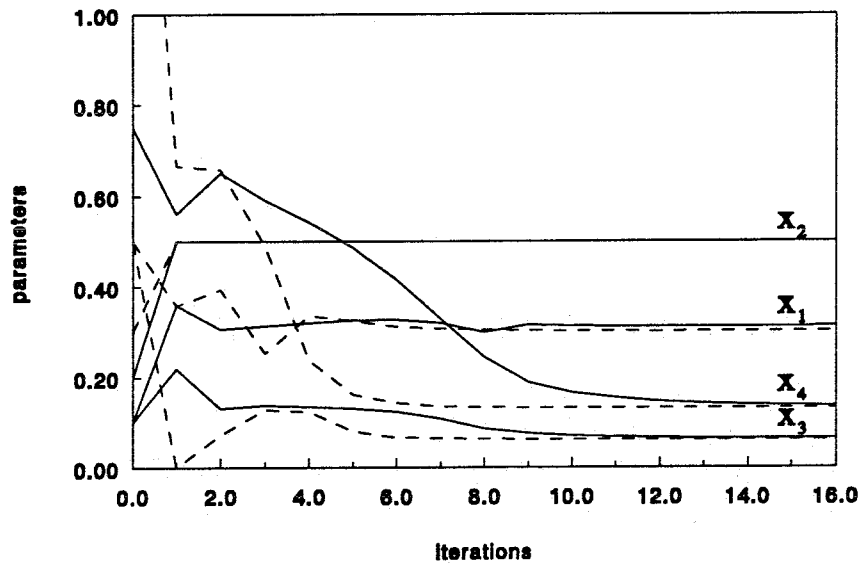Repeating the experiment for $\alpha^* = 0°$ (the asterisk is added to stress the difference between the

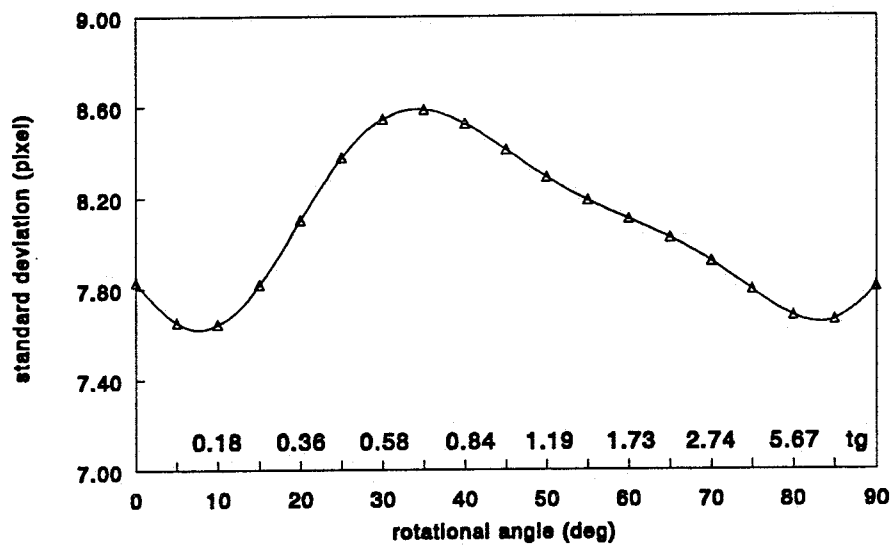*Figure 4.3: parameter estimation with two different initial guesses*

Figure 4.4: standard deviation of the residual field as function of α

experimental design parameter α and its estimated value) leads to more peculiar results. Again starting from both intial guesses the parameters converge. This time α is estimated -16.7°. In addition different values are found for the remaining parameters (tabel 4.3). Loading an identical specimen according to test 3 ("confined" testing) α becomes 31°. This again may be the fiber direction, but surely this is just a guess considering the parameter values.

Uniaxial tests (test 2) for $\alpha^* = 0°$ and $\alpha^* = 45°$ show convergence of parameters. Since these tests malfunction in numerical simulations, interpretation of the results becomes even more difficult. For $\alpha^* = 0°$ the angle of material symmetry is estimated between 37.6° and 37.9°. This is consistent with the above estimated $\beta = 75.5°$. On the other hand parameter values do not agree with those of the biaxial test.

A typical identification feature appears analysing the uniaxial test for $\alpha^* = 45°$. From the second initial guess, stiffness ratio E_1/E_2 is estimated larger than 1. If the E_2 direction is defined as stiffest (fiber) direction, this means transformation of parameters is needed. This results in $\alpha = 22°$.

Tabel 4.3: parameter estimation results

Model	Results *(starting from initial guess 1)*					Results *(starting from initial guess 2)*				
	S.D.	Ě	v	Ǧ	tg(α)	S.D.	Ě	v	Ǧ	tg(α)
SQUARE S. ($\alpha^* = 0°$)										
test 2	5.018	0.359	0.123	0.162	0.769	5.019	0.388	0.125	0.174	0.778
test 3[1]	4.983	0.102	0.499	0.060	0.600	4.984	0.090	0.499	0.059	0.586
test 4[1]	6.761	0.127	0.151	0.200	-0.29	6.742	0.109	0.304	0.182	-0.30
($\alpha^* = 20°$)										
test 2	8.804	0.031	0.177	0.073	1.908	9.768	0.605	0.499	0.947	0.670
($\alpha^* = 45°$)										
test 2	8.058	0.001	0.499	0.015	0.406	5.304	16.37	0.119	0.470	-2.49
test 2[2]						5.304	0.061	0.119	0.029	0.402
test 3	4.886	0.015	0.499	0.039	0.336	4.672	1.514	0.499	0.063	-0.13
test 3[2]						4.672	0.661	0.499	0.042	7.513
test 4	7.724	0.313	0.499	0.065	0.136	7.624	0.303	0.499	0.062	0.133
TRAPEZIUM S. ($\alpha^* = 45°$)										
test 2	10.84	0.028	0.499	0.016	0.637	10.68	0.024	0.499	0.016	0.641

[1] *Second initial guess: Q set to $[0.1, 0.1, 0.1, 0.1]$.*
[2] *Second initial guess: after transformation.*

Two more experiments are discussed: a uniaxial test of a trapezium shaped specimen ($\alpha^* = 45°$) and a uniaxial test of a square specimen for $\alpha^* = 20°$. Both experiments give different sets of

parameters, estimating $\alpha = 32.5°$ in case of the trapezium specimen (almost similar to the estimated angle for $\alpha^* = 0°$ and test 3) and $\alpha = 62.3°/33.8°$ for the $\alpha^* = 20°$ test. In particular the performance of the latter experiment is disapproved.

4.5 DISCUSSION

The above results of the parameter estimation do not look good. However, it would be wrong to conclude that the identification method failed. Firstly, the experimental data are reliable and do not contain large measurement errors. By using the local approach, model errors due to geometry and boundary condition measurement are acceptable. Secondly, in all cases the standard deviation of the residual is minimized to approximately the measurement error deviation. This means that the estimation algorithm works like we would expect.

Small deviations in the estimated angle of material symmetry can be caused by inaccuracies in specimen preparation. Moreover, it is possible that α is sensitive for deformation of the specimen (non-linear behavior). The deflections we found however can not be explained in this way, nor can the difference in material parameters. Yet we should seek the solution of our problem in the estimation of the angle of material symmetry. The residual as function α shows two minima between (in the studied case) $0°$ and $90°$. This indicates that the assumption of ordinary orthotropic behavior in section 4.2.1 is not correct.

Analyzing the material structure, the application of an angle ply laminate model, consisting of *two* orthotropic laminas is more appropriate. The strain-stress relationship of such model is described by an identical matrix $S^* = T^TST$ (eq. 3.1), the elements however, depend in a different way on the material parameters of one lamina than assumed in the simple orthotropic model. Hence the results from parameter estimation lead to the best possible approximation of matrix S^*, but the material parameters including α can not be interpreted correctly.

It will be clear that a generalization of the conclusion of the numerical simulation, based on the present results is hard to do. Since the parameters and in particular α can not be validated, it becomes difficult even to comprehend which experiment actually is performed (in the light of the simulations). A better model could give the solution of this problem.

4.6 CONCLUSIONS

The assumption of plane orthotropic behavior complicates the results of this chapter. The identification method relies on a suitable combination of experiment and model. The estimation of parameters will feature large deviations if one of two facets is not compatible with the other. This propably is the case for our experiments. The measurements are set-up carefully and give good

results. The model used to describe the material behavior finally leads to bad results. The estimation algorithm still minimizes the residual field.

Recommendations are:

- Comparison of the used orthotropic model and the laminate model can give information about the real material parameters.
- Measurement data can be re-used to estimate material parameters in the laminate model.

5

General discussion, conclusions and recommendations

The presented study aimed at finding a suitable testing configuration for membranes with orthotropic properties and high stiffness ratios. The outcome of the simulations proved that searching for such configuration is justifiable. The systematic analysis of the nature of applied strain fields and the results of parameter estimation pointed out that nonuniform strain distributions contain more information about material parameters than uniform strain fields. Because biaxial tests resulted in inhomogeneous strain fields, these models have shown a good identifiability. Dealing with high stiffness ratios meant, that the angle of material symmetry became an important experimental parameter. In a suitable configuration, this angle had to be chosen different from the loading direction to gain good results. Specimen geometry seemed less important.

A number of problems arised in the experiments, that could not be simulated. The assumption of linear elastic orthotropic behavior of the specimen material, expressed by a similar model choise in the finite element calculations, has proved to be uncorrect. This has been found out by looking at residuals and parameter values in the light of background knowledge. Since model errors were not account for in the simulations, the conclusions for chapter 3 could not be validated.

The conclusions based on the simulations are valiable. The conclusions based on the experiments must be used to come to better experimental results. An important recommendation is to change the numerical model in a more appropriate model, for instance the angle ply laminate model. In general, we must become more aware of the possibility of model errors and gain more insight in the way these appear in the estimation process.

References

Borst, R. de, Kusters, G.M.A., Nauta, P., Witte, F.C. de, 1985, "DIANA - A comprehensive, but flexible finite element system", in "Finite Element Systems; a handbook", ed. C.A. Brebbia, Springer Verlag, Berlin, New York and Tokyo.

Chamis, C.C., Sinclair, J.M., 1977, "Ten degree off-axis test for shear properties in fiber composites", in "Experimental Mechanics", pp 339-346.

Courage, W.M.G., Hendriks, M.A.N., 1989, "Module Parest", Internal reports WFW 89.38 and WFW 89.39, in Dutch, Eindhoven University of Technology, The Netherlands

Hendriks, M.A.N., 1991, "Identification of the mechanical behavior of solid materials", Ph.D.-thesis, Eindhoven University of Technology, the Netherlands.

Norton, J.P., 1986, "An introduction to identification", Academic Press, New York and London.

Peters, G.W.M.P., 1987, "Tools for the measurement of stress and strain fields in soft tissue", Ph.D.-thesis, University of Limburg, the Netherlands.

Roddeman, D.G., 1988, "Force transmission in wrinkled membranes", Ph.D.-thesis, Eindhoven University of Technology, the Netherlands.

Zamzow, H., 1990, "The Hentschel random access tracking system HSG 84.30", in "Proceedings of the symposium on image based motion measurement", La Jolla, California, USA, ed. J.S. Walton, SPIE, Vol. 1356, pp.130-133.